Am J Physiol Gastrointest Liver Physiol 292: G1695–G1705, 2007.
First published March 8, 2007; doi:10.1152/ajpgi.00209.2006.

Measurement of liver collagen synthesis by heavy water labeling: effects of profibrotic toxicants and antifibrotic interventions

James L. Gardner,[1] Scott M. Turner,[1] Abraham Bautista,[1] Glen Lindwall,[1] Mohamad Awada,[1] and Marc K. Hellerstein[2,3]

[1]*KineMed, Inc., Emeryville;* [2]*Department of Nutritional Sciences and Toxicology, University of California, Berkeley; and* [3]*Department of Medicine, San Francisco General Hospital, University of California, San Francisco, California*

Submitted 12 May 2006; accepted in final form 2 February 2007

Gardner JL, Turner SM, Bautista A, Lindwall G, Awada M, Hellerstein MK. Measurement of liver collagen synthesis by heavy water labeling: effects of profibrotic toxicants and antifibrotic interventions. *Am J Physiol Gastrointest Liver Physiol* 292: G1695–G1705, 2007. First published March 8, 2007; doi:10.1152/ajpgi.00209.2006.—Enhanced production of collagen is central to fibrotic disorders such as hepatic cirrhosis and pulmonary fibrosis. We describe a sensitive, quantitative, and high-throughput technique for measuring hepatic collagen synthesis in vivo through metabolic labeling with heavy water (^2H_2O). Rats and mice received ^2H_2O in drinking water for up to 35 days. Deuterium incorporation into collagen-bound amino acids (AA) alanine and hydroxyproline (OHP) was measured by gas chromatography-mass spectrometry. A threefold stimulation of collagen fractional synthesis was observed under the maximum dosage of carbon tetrachloride (CCl_4; 1.67 ml/kg). Deuterium enrichment was systematically 20% higher in AA from monomeric collagen relative to dimeric collagen, consistent with slower turnover of the latter. Administration of 1% griseofulvin to mice resulted in a significant, threefold increase in liver collagen synthesis, observable within 12 days and consistent with predicted interstrain differences (C57/Bl6J > BALB/c). Deuterium enrichments of OHP from total liver proteins correlated well with alanine or OHP from isolated collagen. Fibrogenesis subsided after withdrawal of CCl_4 exposure and was reduced to various degrees by coadministration of interferon-γ, rosiglitazone, atorvastatin, or enalapril. Changes in isotopically measured collagen synthesis correlated with, but were more sensitive and reproducible than, standard histological staining (trichrome) for fibrosis. In summary, liver collagen synthesis can be measured sensitively and with high precision over a short time period, without radioactivity, thereby providing a relatively high-throughput in vivo strategy for rapidly measuring profibrotic activities of suspected hepatotoxicants and antifibrotic activities of drug candidates.

fibrogenesis; hydroxyproline; in vivo; strain differences

THE TRANSIENT ACCUMULATION of collagen in tissues is a normal feature of wound repair (35). Fibrosis, the pathological buildup of extracellular matrix proteins, stems from prolonged tissue injury, such as from chronic exposure to toxicants, irritants, or mechanical stress, as well as infection, inflammation, or oxidative stress. Fibrosis may ultimately result in organ failure (6, 35, 34).

The hepatic stellate cell (HSC) is the primary source of collagen in liver (14) and becomes rapidly activated by cytokines at the onset of wound response (36). HSC activation is an active focus of drug intervention studies for liver fibrosis. Certain cytokines, such as interferon-γ (IFN-γ), and peroxisome proliferator-activated receptor-γ (PPARγ) agonists, such as rosiglitazone, are capable of reducing experimental fibrosis (2, 15).

Although the complex mechanisms of wound repair and fibrosis are increasingly well understood, effective antifibrotic treatments are lacking (6). One problem is that sensitive markers of fibrogenesis have not been available. Biochemical measurement or histological staining of collagen content suffers from important limitations, since liver collagen accumulation typically occurs over a long time frame and exhibits considerable variability among animals. Even in experimental models, large groups of animals must be treated for weeks or months to assess the efficacy of various interventions.

This problem of insensitive outcome metrics is common in conditions characterized by large, relatively slow-turnover pools (9, 21). Drug-induced alterations in collagen production or degradation may be masked by the large background of collagen that is present in tissue. As discussed elsewhere by Hellerstein and colleagues (18, 40), a solution to this problem exists, in principle, through the measurement of the dynamics (i.e., the synthesis rate) of collagen, rather than its pool size. Small differences in the rate of addition of newly synthesized collagen molecules can be observed immediately and with great sensitivity, independently of the pool size or turnover rate of collagen that is already present.

We describe a stable isotope/mass spectrometric technique utilizing heavy water (^2H_2O) labeling for measuring the synthesis rate of tissue collagen in vivo. The heavy water labeling approach is extremely sensitive and reproducible for measurements of the kinetics of slow-turnover proteins like collagen (9, 40). The method involves brief treatment regimens, modest to moderate doses of toxicant, and small numbers of animals. We corroborate previous observations regarding the influence of intermolecular cross-linking on collagen turnover and show the fibrogenic response to toxicant exposure to be quantitatively dependent on strain, species, concentration, and time. The technique has high analytic reproducibility. Finally, suppression of fibrogenesis by known antifibrotic agents and test compounds is shown to be reproducible and more sensitive than static metrics of collagen content, thus offering the potential for efficient new applications in drug discovery.

MATERIALS AND METHODS

Materials. Collagen standards and collagen antibodies were obtained from Rockland Immunochemicals (Gilbertsville, PA). ^2H_2O was obtained from Spectra Stable Isotopes (Columbia, MD). Mouse

Address for reprint requests and other correspondence: M. K. Hellerstein, Dept. of Nutritional Sciences and Toxicology, Univ. of California, Berkeley, CA 94720 (e-mail: march@nature.berkeley.edu).

The costs of publication of this article were defrayed in part by the payment of page charges. The article must therefore be hereby marked "*advertisement*" in accordance with 18 U.S.C. Section 1734 solely to indicate this fact.

recombinant IFN-γ was obtained from United States Biological (Swampscott, MA). Rosiglitazone was obtained from GlaxoSmith-Kline (Research Triangle Park, NC). Ketoconazole was obtained from Chimes Pharmacy (Berkeley, CA). Enalapril and atorvastatin were obtained from Pfizer (New York, NY). Other reagents were obtained from Sigma Chemical (St. Louis, MO), unless otherwise specified.

Animals and protocols. Sprague-Dawley (SD) rats (200–300 g; Simonsen Labs, Gilroy, CA), C57/Bl6J mice (16–18 g; Jackson Laboratories, Bar Harbor, ME), and 129X1/SVJ, BALB/c, and Swiss Webster (CW) mice (Charles River Laboratories) were used for these studies. All animals were housed in specific pathogen-free vivariums with controlled light-dark cycle, temperature, and humidity. Cages, bedding, food, and water were autoclaved before use. Housing was in groups of five mice per cage or two rats per cage. Rats and mice were housed in separate rooms. Unless otherwise stated, all feeding was ad libitum with Purina rodent chow. All studies received prior institutional approval.

Animals received up to 1.67 ml/kg CCl_4 in olive oil intraperitoneally twice per week for up to 35 days. Dietary griseofulvin (1% wt/wt in AIN-93 diet; Research Diets, New Brunswick, NJ) was administered to mice for 12 days. Mice received IFN-γ at 50,000 U/day intraperitoneally. Dietary rosiglitazone (0.053 g/4,057 kcal in AIN-93M diet) was administered to CW mice for 14 days. Vitamin E was administered in olive oil vehicle at a concentration of 250 $mg \cdot kg^{-1} \cdot day^{-1}$ (370 IU/kg) per os. Enalapril or atorvastatin were given in drinking water vehicle at 20 $mg \cdot kg^{-1} \cdot day^{-1}$ per os. Animals were anesthetized with isoflurane. While under anesthesia, animals were killed and blood was withdrawn by cardiac puncture followed by severing of the diaphragm as performed previously (41).

A ^2H_2O-labeling protocol was performed as described previously (26, 41, 10). Briefly, an initial priming dose of 99.8% ^2H_2O in 0.9% NaCl was given via intraperitoneal injection to achieve ~5% body water enrichment, followed by administration of 8% ^2H_2O in drinking water for up to 35 days. Rodents have previously been maintained on chronic ^2H_2O intake at up to 30% enrichment in drinking water without effects on growth, food intake, behavior, activity, or fertility (22). Consistent with these reports, no adverse effects were observed in animals receiving 8% ^2H_2O.

Sample preparation. Livers were excised and flash frozen in liquid nitrogen. Frozen tissue was shattered by mortar and pestle. Approximately 20 mg of tissue were then homogenized at 4°C with either a Polytron model PT 10-35 tissue tearor or a MiniBeadbeater-96 (Biospec, Bartlesville, OK) bead mill with 0.7-mm zirconium silica beads. For bead mill homogenizations, samples were subjected to three cycles of 40 s per cycle and placed on ice for 1 min between cycles.

For total protein isolation, homogenizations were performed in pure, deionized water. Four volumes of acetone at −20°C were added to 1 volume (450 μl) of the tissue homogenate. The material was centrifuged at 15,000 *g* at 4°C for 15 min, and the resulting pellet was washed by brief vortexing with 1 volume of 95% ethanol at −20°C. After centrifugation, the supernatant was removed, and the pellet was dried under vacuum.

Collagen extract was prepared by performing homogenizations in 450 μl of 100 mM NaOH. Under these conditions, collagen remains insoluble whereas most other proteins are readily dissolved (32, 33). After centrifugation at 7,000 *g* for 10 min at 4°C, the supernatant was removed, and the pellet was briefly vortexed in 500 μl of H_2O. After centrifugation, the supernatant was removed, and the pellet was dissolved in 5 μl of SDS-PAGE sample buffer containing 5% (vol/vol) β-mercaptoethanol and 4 M urea (Bio-Rad, Hercules, CA). After boiling for 3 min, the dissolved material was size-fractionated by 7.5% SDS-PAGE. With the use of standard techniques, proteins were subsequently transferred onto polyvinylidene difluoride (PVDF). Protein bands representing monomeric and dimeric collagen were routinely identified by comigration with standards. Protein bands that corresponded to collagen were cut from the resulting membrane after the membrane was stained with brilliant blue R-250.

Preparation of analytes for mass spectrometric analyses. Acetone-precipitated total tissue protein or excised PVDF-bound proteins were hydrolyzed by incubation in 6 N HCl at 110°C for 16 h as previously described (28). Hydrolysates were dried under vacuum and then suspended in 1 ml of 50% acetonitrile, 50 mM K_2HPO_4, pH 11. Twenty microliters of pentafluorobenzyl bromide (Pierce) were added, and the sealed mixture was incubated at 100°C for 1 h. Derivatives were extracted into ethyl acetate, and the top, organic layer was removed and dried by addition of solid Na_2SO_4 followed by vacuum centrifugation. To acetylate the hydroxyl moiety of hydroxyproline, we subsequently incubated samples with 50 μl of methyl imidizole and 500 μl of acetic anhydride for 15 min at room temperature. Alternatively, acetic anhydride was replaced with 100 μl of *N*-methyl-*N*-(*tert*-butyldimethylsilyl)trifluoroacetamide (Pierce), and the material was sealed and incubated at 100°C for 30 min. This material was extracted in a biphasic system of water and petroleum ether and subsequently dried with Na_2SO_4 and lyophilized before analysis. Care was taken to remove all water, to prevent generation of chromatographic contaminants. The method of analyte preparation was adapted for use in a 96-well format by using a cyclic olefin copolymer (COC/TOPAS) Multi-Tier plate (Biotech Solutions, Mount Laurel, NJ) with 2-ml flat-bottom glass inserts and a poly(tetrafluoroethylene)-coated butyl molded mat. For this approach, organic phases containing derivatized material were rendered anhydrous by passing the organic phase over 1.85 g of anhydrous Na_2SO_4, placed in each of the wells of a Whatman Unifilter GF/F deep-well filter plate. Organic solvent and analyte that flowed through the Na_2SO_4 were collected and analyzed by gas chromatography-mass spectrometry (GC-MS).

GC-MS analysis of derivatized amino acids. Using negative chemical ionization (NCI), derivatized amino acids (AA) were analyzed on a DB225 gas chromatograph column (9, 13). The starting temperature was 100°C, increasing 10°C per minute to 220°C. The mass spectrometry used NCI with helium as the carrier gas and methane as the reagent gas. For hydroxyproline (OHP), selected ion monitoring was performed on mass-to-charge ratios of 352, 353, and 354, which are the primary fragment ions for the most abundant isotopomers of the pentafluorobenzyl-*N*,*N*-di(pentafluorobenzyl)acetylprolinate derivative. Alternatively, selected ion monitoring was performed with the mass-to-charge ratios of 445, 446, and 447 for the pentafluorobenzyl-*N*,*N*-di(pentafluorobenzyl)-*N*-methyl-*N*-(*tert*-butyldimethylsilyl) trifluoroacetylprolinate derivative. For alanine, the mass-to-charge ratios of 448, 449, and 450 were monitored for the pentafluorobenzyl-*N*,*N*-di(pentafluorobenzyl)alaninate derivative. In all cases, these mass-to-charge ratios represented the primary daughter ions that included all of the original hydrocarbon bonds from the given amino acid. ^2H enrichment was calculated as described previously (13).

Mole percent excess (MPE) M+1 enrichment (EM_1) and fractional synthesis (f) were calculated as described below and as previously described for alanine (9, 20, 21). The number (n) of exchanging hydrogen atoms in OHP that were derived from body water was calculated by mass isotopomer distribution analysis (MIDA) based on the EM_2/EM_1 ratio, as described previously (9, 10).

Identification of isolated proteins. PVDF-bound collagen standards and rat liver isolates were analyzed for immunoreactivity using rabbit anti-type I collagen antibodies (1:200,000 dilution) or anti-type III collagen antibodies (1:100,000 dilution). A secondary mouse anti-rabbit horseradish peroxidase-linked antibody was used at a dilution of 1:10,000, and ECL Plus (Amersham Biosciences, Uppsala, Sweden) was used to detect binding.After size fractionation by SDS-PAGE, collagen bands were excised, subjected to trypsin degradation, and submitted for peptide identification (AmProx, Carlsbad, CA). Products of trypsin degradation were identified by tandem mass spectrometry and matched to sequence information in the SWISSPROT database.

Analysis of ^2H_2O enrichment in body water. Measurement of ^2H_2O enrichment in body water was carried out as previously described (9,

26) using a Series 3000 cycloidal mass spectrometer (Monitor Instruments, Cheswick, PA).

Histopathology. Saline-perfused liver tissue was fixed in 10% formalin overnight and stored in 70% ethanol. The liver tissue was processed through graded alcohols, cleared in xylene, and infiltrated and embedded into paraffin. Two 4-μm sections were cut; one was stained with hematoxylin and eosin, and the other with Masson's trichrome. Images (3–4 per liver) were captured of the Masson's trichrome-stained sections by using a ×2.5 objective with a Zeiss Axiocam HR 42-RGB camera, converted to 24-RGB, and pieced together in Adobe Photoshop. Compiled images were analyzed with ImagePro-Plus v.5.1 with the use of a custom subroutine to extract the total tissue area (red, blue, and purple colors on a white background) and the areas of fibrosis (blue, blue-gray, and blue-purple). Color segmentation was preset and applied to the images after filtering, with adjustable selections to account for stain variation. The fibrotic area divided by the tissue area yielded the fraction of fibrous tissue within each liver. Resultant images representing the calculated fibrosis were produced to demonstrate the algorithm accuracy.

Samples were also analyzed by Probetex (San Antonio, TX) and scored for degree of fibrosis. Scoring was 0 to 4 with the following descriptions: 0, absence of fibrosis; 1, increased subendothelial staining restricted to central vein and periportal areas; 2, fibrous portal expansion; 3, bridging fibrosis; and 4, cirrhosis with loss of typical lobular architecture. Twenty to forty lobules were assessed per each tissue sample. In addition, slides were scored for necrosis, appearance of inflammatory infiltration, and appearance of mitotic figures in five fields at ×20 magnification.

Statistics. Means and standard deviations (error bars) of treatment groups ($n = 3$ or greater) were compared with Student's *t*-test for statistical significance of pairwise comparisons. Analysis of variance was used for assessing statistically significant differences among more than two groups. Spearman nonparametric correlation served to test similarity among groups. Statistical significance was defined as a P value <0.05. Using SigmaPlot, we fitted f values to a single exponential equation, $f_t = f_{max} \times (1 - e^{-kt})$, and goodness of fit was evaluated using the calculated coefficient of determination (R^2). Variation among replicates was used to calculate an average intra-assay precision of total protein OHP ^2H enrichment data. Replicate groups of animals, three to five in number, were handled simultaneously with an identical treatment regimen. Coefficients of variation (CV) from each group were used to calculate the mean and median intra-assay CV.

RESULTS

Model of deuterium incorporation into collagen-bound nonessential AA, including OHP. After ^2H_2O labeling, tissue collagen synthesis was measured based on incorporation of deuterium into nonessential AA (alanine or OHP) bound to tissue collagen. One approach was to recover the alanine or OHP from isolated collagen; alternatively, OHP was recovered from total tissue protein. The latter approach eliminates the need for collagen isolation and measures turnover of the total collagen pool in a tissue, rather than physically isolating the particular collagen molecules. To properly interpret metabolic incorporation of deuterium atoms from ^2H_2O into biosynthetic end products, such as DNA, lipids, or proteins (9, 10, 25, 26, 37, 41), it is necessary to characterize the number of covalent C–H bonds derived from tissue water in newly synthesized molecules in vivo. Our group (9, 13) has previously discussed the incorporation patterns of ^2H_2O into C–H bonds of nonessential AA such as alanine and glycine. Similarly, protein-bound proline, and hence OHP, can derive from de novo synthesis, diet, or reutilization of degraded tissue proteins (4). Figure 1 depicts routes of deuterium incorporation into alanine and proline via scavenging and biosynthetic pathways, followed by incorporation of either AA into collagen. Posttranslational hydroxylation of roughly one-third of the preprocollagen-bound proline residues produces OHP, an abundant AA that is specific for collagen. Deuterium incorporation in OHP isolated from total tissue proteins may then serve as a quantitative indicator of total collagen turnover in the tissue.

Measurement of collagen fractional synthesis rates based on collagen-alanine in rats and mice. Preparative SDS-PAGE of collagen from rat liver tissue is shown in Fig. 2*A*. The lowermost electrophoretic band from the rat liver preparation comigrated with the α2(I) band of collagen type I standard. Sequences of eight tryptic fragments corroborated the identity of this protein (Table 1). Immunoblot analysis with anti-type I and anti-type III collagen antibodies revealed cross-reactivity with collagen standards and with the collagen type I band from liver preparations, but there was no indication of collagen type III presence in liver preparations (data not shown).

Fractional synthesis of liver collagen in normal mouse and rat was measured during 3–4 wk of continuous ^2H_2O administration, based on deuterium enrichments in collagen-bound alanine. Label incorporation curves reached plateau values (Fig. 2*B*). The exchangeable number of hydrogens in covalent C–H bonds in alanine was determined by MIDA of the labeling pattern in alanine to equal 4, i.e., representing complete equilibration with tissue H_2O, as shown previously (9, 13). By using this value ($n = 4$) to calculate asymptotic enrichments, a plateau of ~37% new collagen was reached in both species. These results suggest the existence of a subpopulation of collagen that is replaced at a much slower rate than the pool undergoing label incorporation (19). The replacement rate constant for the rapid turnover pool of collagen in mice (129X1/SVJ strain) was roughly twice the rate in SD rats, 13.6 and 7.3% per day, respectively (Fig. 2*B*).

Correlation between enrichments of monomeric vs. dimeric collagen. Preparative SDS-PAGE of mouse liver collagen allowed separation of collagen variants by isoform and cross-linking. A systematic difference was observed between monomeric type I collagen (roughly 20% more enriched) and dimeric collagen from the same liver samples (Fig. 3). This observation held for both collagen-bound alanine and collagen-bound OHP. The systematically lower enrichment of dimeric relative to monomeric collagen is in keeping with reports of increased proteolytic susceptibility and thus more rapid turnover of monomeric collagen relative to cross-linked collagen (1, 38, 42).

Fractional synthesis of collagen-bound alanine in rodents in response to CCl_4. Hepatic fibrogenesis in response to CCl_4 in SD rats (Fig. 4) was first determined on the basis of label incorporation into monomeric collagen-bound alanine. A statistically significant difference between the untreated and CCl_4-treated groups was observed starting at 2 days and continuing through termination of the study (*day 28*). In control animals, the value for f was 35.6 ± 6% new collagen after 28 days; this was surpassed at 14 days of CCl_4 treatment at either CCl_4 dose (42.3 ± 12.3% new collagen at 1 ml/kg and 47.6 ± 7.6% new collagen at 1.67 ml/kg). After 28 days of CCl_4 administration (1 ml/kg), 79.4 ± 9.4% of collagen was newly synthesized. Histopathological examination of tissues (Colorado Pathol-

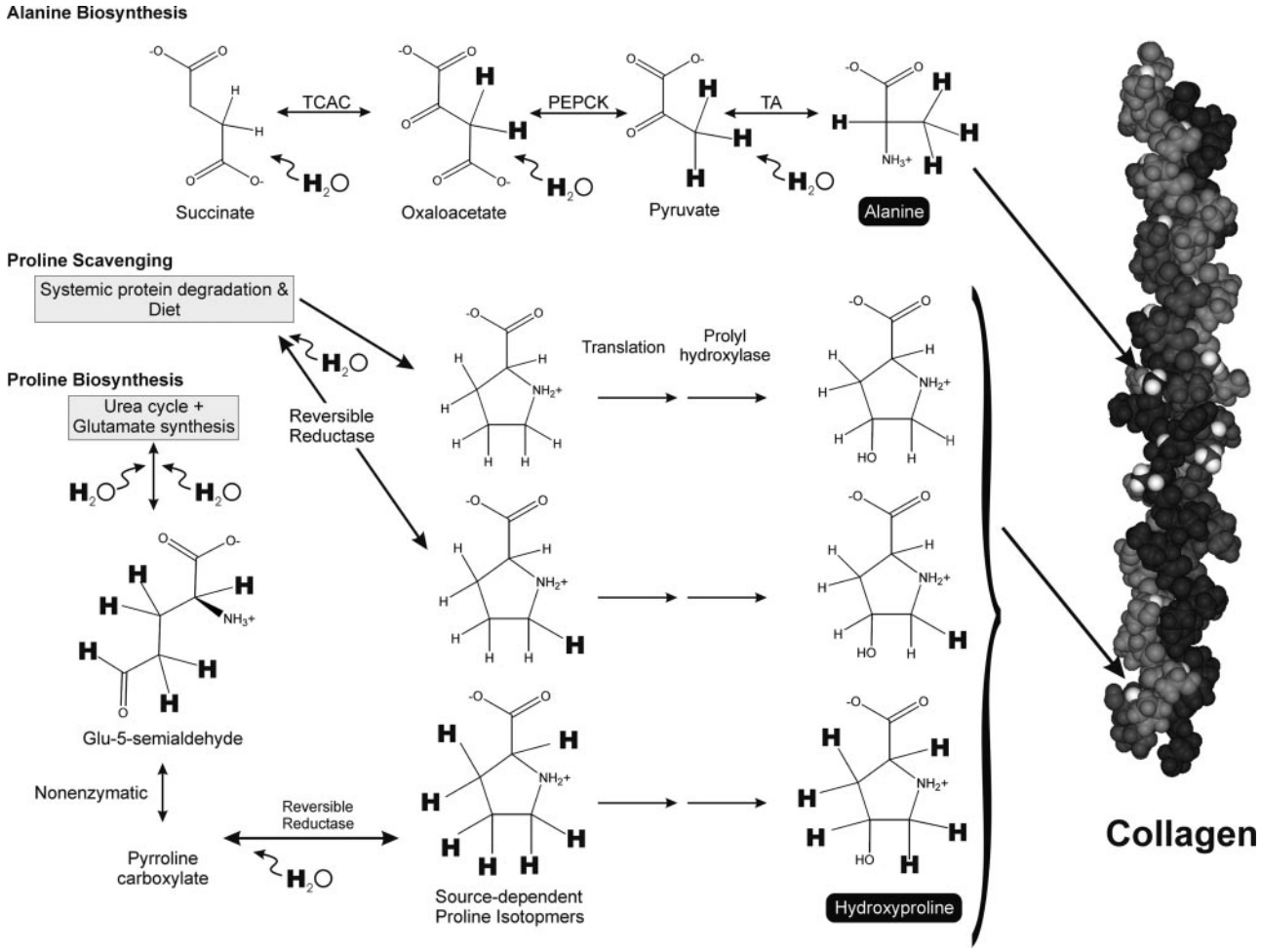

Fig. 1. Deuterium, depicted as a bold "H," is incorporated from heavy water into amino acid residues of nascent fibrillar collagen. Alanine (Ala) exhibits classically nonessential metabolism, arising biosynthetically from abundant metabolic precursors, in particular from the tricarboxylic acid cycle (TCAC), phosphenolcarboxykinase (PEPCK), and transaminase activity (TA), yielding $n = 4$ for incorporation of deuterium into C–H bonds. Proline and, hence, hydroxyproline (OHP) are nonessential amino acids but exhibit a high degree of essentiality, being scavenged from systemic protein degradation and diet. This results in 3 major isoptomers of OHP possibly coexisting in collagen: *1*) fully deuterated from biosynthesis, *2*) singly deuterated, scavenged proline via reversible δ-1-pyrroline-5-carboxylate reductase, and *3*) nondeuterated scavenged proline. The space-filling model of fibrillar trimeric collagen was adapted from Protein Data Bank accession no. 1BKV. Each peptide chain is depicted in light gray, dark gray, or charcoal, and potential sites of deuterium substitution in Ala and OHP are depicted in white.

ogy Services, Collbran, CO) revealed "minimal fibrosis" and increased staining via Mason's trichrome in 1 ml/kg CCl_4-treated rats throughout the time course of treatment.

Asymptotic ^2H enrichment of OHP. Enrichment of collagen-bound alanine and OHP was determined concurrently from untreated and 1.0 ml/kg CCl_4-treated SD rats. There was a good correlation between these AA, with no observable change in the relationship during CCl_4 treatment (Fig. 5*A*). Average values are plotted for EM_1(OHP)/EM_1(ALA) from each treatment group (Fig. 5*B*). The correlation was very close ($R^2 = 0.813$). Interestingly, OHP enrichments were well below theoretical maxima, indicating that many of the C–H bonds in newly synthesized proteins had not incorporated deuterium from ^2H_2O. Fractional synthesis values from collagen-OHP and collagen-alanine were equivalent when asymptotic OHP enrichments (A_1^∞) of ~1.1 × body ^2H_2O enrichment were used. This represents about 1.5 C–H bonds incorporating ^2H in new OHP. There is a theoretical maximum of six new hydrogen atoms in OHP (Fig. 1). Thus there appears to be a dilution of prolyl-tRNA pools by preexisting (unlabeled) proline (Fig. 1), as reported previously in avian models (4). Importantly, the mass isotopomeric pattern in OHP, which reflects the number of exchanging hydrogens in those proline residues that did in fact derive from de novo synthesis (10), was stable across treatment groups. These MIDA calculations confirm that the different treatments tested did not influence the number of exchanging hydrogens in newly synthesized proline in prolyl-tRNA.

Comparison among the three metrics of collagen synthesis. Synthesis values were compared for alanine from isolated collagen, OHP from isolated collagen, and OHP from total tissue protein. It should be noted that kinetics for isolated collagen and total protein OHP are not expected to be identical, because the latter encompasses all collagens, whereas the former specifically represented the monomeric type I collagen that was isolated. CCl_4 was administered to rats for 7–35 days, but administration of ^2H_2O was limited to the final 7 days preceding euthanasia. Administration of 1.0 ml/kg CCl_4 to SD rats resulted in a rapid increase in liver collagen synthesis (Fig.

6), with significant differences ($P < 0.05$) relative to controls by *day 14* for collagen-alanine and collagen-OHP. Synthesis based on total protein-OHP rose after 7 days and remained elevated thereafter. After 35 days, all methods revealed ~70% new collagen synthesized per week. According to a Spearman rank order correlation, the following coefficients were observed: 0.770 for collagen-alanine vs. collagen-OHP, 0.683 for collagen-OHP vs. protein-OHP, and 0.618 for collagen-alanine vs. protein-OHP ($P < 0.001$ in all cases). These results confirm that deuterium incorporation into total tissue protein-OHP represents a technically simpler approach that reflects changes in deuterium incorporation into collagen-bound AA.

Strain differences in mice for fibrogenic response to hepatotoxicants. To explore potential differences among mouse strains for fibrogenesis, we conducted dose-response and time course experiments, using two profibrotic agents and four strains of mice (Fig. 7). 129X1/SVJ and CW mice received increasing doses of CCl_4. In 129X1/SVJ mice given 0, 0.25, and 1 ml/kg CCl_4 concurrently with 21 days of continuous ^2H_2O intake, a significant increase in *f* in total protein-OHP was observed only for the 1 ml/kg CCl_4 treatment groups after 14 days (Fig. 7*A*) compared with controls.. In contrast, CW mice exhibited (Fig. 7*B*) a significant increase in *f* at 7 days at a lower dose of CCl_4 (0.05 ml/kg; 21.6 ± 6.6% in controls vs. 32.1 ± 2.9% in CCl_4-treated mice, $P = 0.014$), and the fibrogenic response increased further with doses of CCl_4 up to 0.3 ml/kg. The C57/Bl6J strain exhibited 1.7-fold higher synthesis of collagen than the BALB/c strain (69.4 ± 11.1 vs. 40.0 ± 11.0% new collagen, $P = 0.013$, Fig. 7*C*) in response to griseofulvin in the diet.

Table 1. *Peptides identified by LC-MS-MS from trypsin digestion of the putative α2(I) band of collagen, isolated by preparative SDS-PAGE*

	Sequence	MH+	BLAST Result
1	(R)P*GPIGPAGPR	933.9	Rat α2(I)
2	(R)GLPGADGRAGVMGP*P*GNR	1712.5	Rat α2(I)
3	(R)GPSGPQGIR	869.0	Rat α2(I)
4	(R)GPP*GAVGSP*GVNGAP*GEAGR	1752.4	Rat α2(I)
5	(R)GAP*GPDGNNGAQGPP*GPQGVQGGK	2147.2	Rat α2(I)
6	(R)GDGGPP*GM*TGFP*GAAGR	1549.7	Rat α2(I)
7	(R)TGPP*GP*SGITGPPGPPGAAGK	1803.9	Rat α2(I)
8	(K)GELGPVGNPGP*AGPAGPR	1616.5	Rat α2(I)

Asterisks indicate +16.00 amu modification of preceding amino acid. Parentheses denote amino acid in the putative α2(I) (PI) position of the trypsin cleavage site. LC-MS-MS, liquid chromotography-mass spectrometry-mass spectrometry.

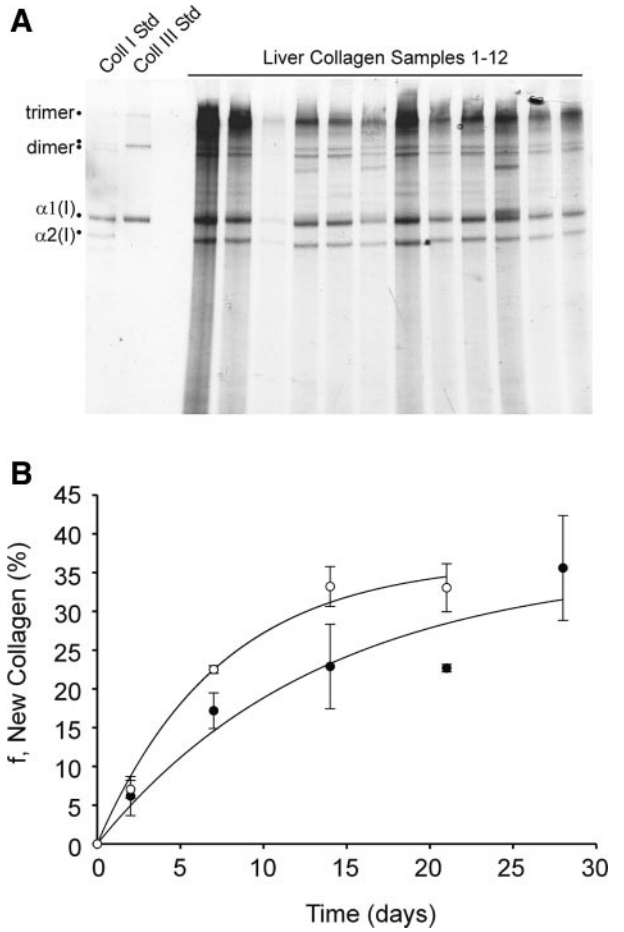

Fig. 2. Kinetics of collagen isolated from the liver tissue of mice and rats. *A*: a representative preparative protein blot of collagens isolated from liver tissue. Monomeric isotypes of type I collagen are indicated using standard nomenclature: isotype 1 is α1(I), and isotype 2 is α2(I). Two dimeric collagens, [α1(I)]2 and α1(I)α2(I), and trimeric collagen, [α1(I)]2α1(I), also are indicated. *B*: fractional synthesis (*f*) of monomeric collagen as measured in terms of excess enrichment (EM_1) in collagen-bound Ala. Reported values are averages with $n \geq 3$ animals per data point, with standard deviation represented by error bars. Exponential curve fits yielded maximal fractional synthesis values of 36 and 37% for rat and mouse, respectively, and rates of 7.3 and 13.6% per day for rat and mouse, respectively. The fitted curves yielded $R^2 = 0.928$ and 0.990 for rat and mouse, respectively.

Histopathological fibrosis and stable isotope-measured fibrogenesis after CCl_4 and toxicant withdrawal or therapeutic interventions. The kinetics of reversal of CCl_4-induced fibrogenesis was evaluated in CCl_4-treated CW mice. The regimens tested were spontaneous recovery, IFN-γ treatment, and treatment with other putative antifibrotic agents. For these studies, a 96-well plate format was used for rapid preparation of tissue homogenates, hydrolysates, and amino acid derivatives, and fibrogenesis was measured by deuterium incorporation into total protein-bound OHP. The spontaneous recovery protocol

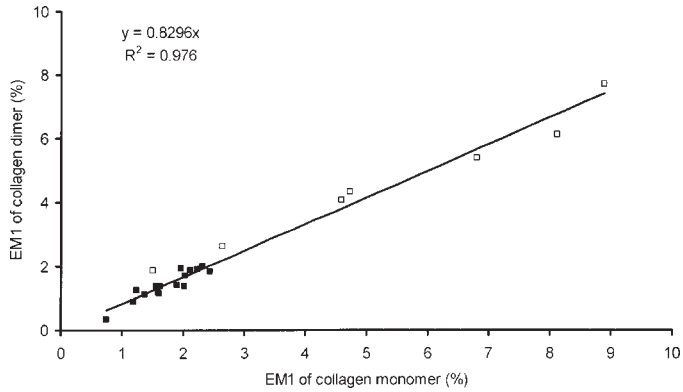

Fig. 3. Dimeric collagen exhibits systematically lower enrichment than monomeric collagen from the same sample. Collagen was isolated from liver tissue of 129X1/SVJ mice, and collagen-bound Ala or OHP were isolated. Correlation between excess enrichments shows that monomeric collagen was 1.2-fold more enriched than dimeric collagen. By forcing a fit through the origin, linear regression is shown for correlation between EM_1 of monomeric vs. dimeric collagen-bound Ala (□, $n = 7$) or OHP (■, $n = 17$).

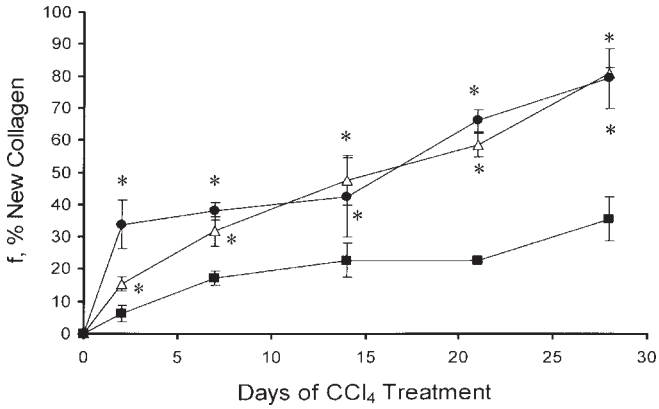

Fig. 4. Relative to untreated control (■), a rise in collagen fractional synthesis appeared after 2 days of 1.0 (●) and 1.67 ml/kg (△) carbon tetrachloride (CCL_4) treatment in Sprague-Dawley (SD) rats. Average fractional synthesis was derived from collagen-bound Ala. Error bars represent standard deviations in each time and treatment combination ($n = 3$ animals per data point). Statistical significance ($P < 0.05$, $n = 3$) was achieved between control and treated groups at each time point as determined by Student's *t*-test between vehicle and control groups (data for vehicle-treated animals are also depicted in Fig. 2).

consisted of two doses of 0.5 ml/kg CCl_4 followed by administration of ^2H_2O after different periods of time (Fig. 8*A*). The ^2H_2O was administered during the final 7 days preceding euthanasia. When measured 7 days after CCl_4 was discontinued, *f* was 34.9 ± 4.8% new collagen per week (Fig. 8*B*). After 14 days, *f* had returned to normal (19.1 ± 2.9% new collagen per week, $P < 0.001$ vs. *day 7*), and values remained low at *day 21* (Fig. 8*B*).

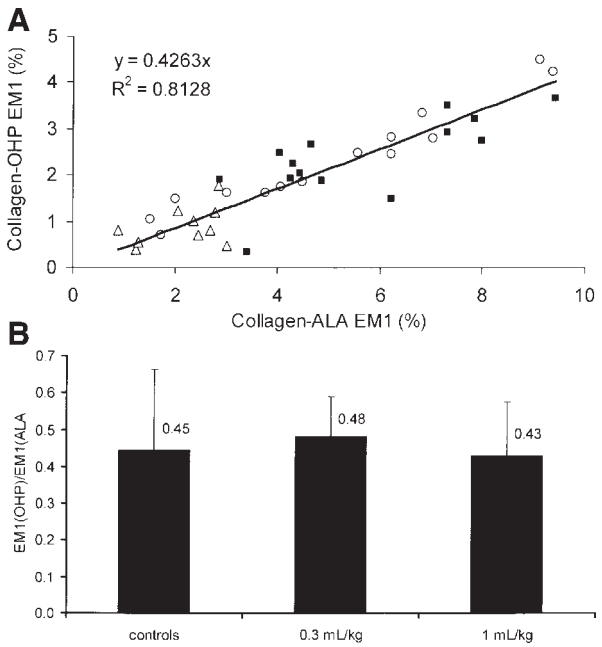

Fig. 5. Relationship between EM_1(Ala) and EM_1(OHP) of both control and CCL_4-treated SD rats. *A*: pairwise correlation between collagen-OHP EM_1 vs. collagen-Ala EM_1 per each sample indicates a consistent relationship of 2.5-fold higher enrichment of Ala relative to OHP. Analysis of samples ($n = 38$) was performed with control (△), 0.3 (○), and 1.0 ml/kg (■) CCL_4-treated SD rats, with no indication of bias as a function of treatment. *B*: an alternative representation of data from *A*, depicted as the average ratio of collagen-OHP EM_1 to collagen-Ala EM_1. No significant difference in this relationship was observed among the 3 CCL_4 treatment groups tested.

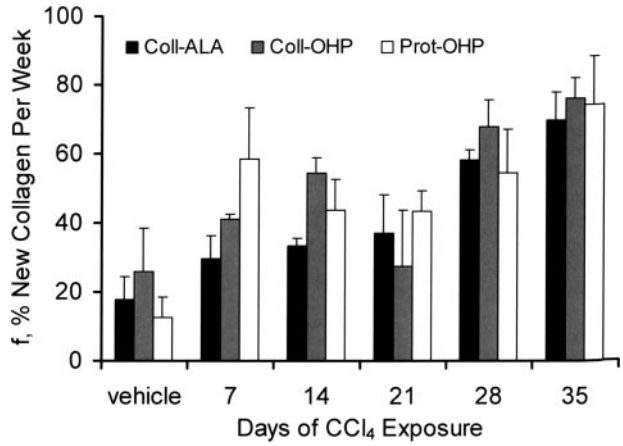

Fig. 6. Three metrics of liver collagen synthesis per week after continuous exposure to CCL_4. SD rats ($n = 3$) were treated for up to 35 days with 1 ml/kg CCL_4 and received ^2H_2O for the last 7 days of treatment. In each sample, fractional synthesis of collagen was measured in collagen-bound Ala (Coll-Ala), collagen-bound OHP (Coll-OHP), and protein-bound OHP (Prot-OHP). In all cases, significance ($P < 0.05$) was reached at *days 28* and *35* relative to vehicle control. The 3 metrics yielded comparable results, through which there was observed a statistically significant ($P < 0.05$), 2-fold rise in weekly collagen fractional synthesis in treated groups vs. vehicle by *day 14*.

Treatment with IFN-γ concurrently with CCl_4 (Fig. 9*A*) partially suppressed fibrogenic response, relative to CCl_4 alone, after 1 wk. Several other agents with hypothesized antifibrotic actions were also tested. Administration of rosiglitazone produced a significant reduction in CCl_4-induced fibrogenesis after 3 wk of coadministration, but not after 2 wk (Fig. 9*B*). Daily oral gavage of high doses of vitamin E did not reduce, but nonsignificantly enhanced, the CCl_4-induced fibrogenic response. Enalapril and atorvastatin exhibited statistically significant, although modest, suppression of CCl_4-induced fibrogenesis after 3 wk of treatment (Fig. 10*A*). Histopathology of the same tissues showed moderate fibrosis in the CCl_4 treatment group, with morphological characteristics of late-term and/or subtoxic liver damage rather than acute toxicity (Fig. 10*B* and data not shown). Figure 10*B* shows fibrosis scoring, demonstrating fibrosis in all groups of CCl_4-treated mice but no significant differences in fibrosis scores among groups that received cotreatment with antifibrotic compounds. All antifibrotic treatment groups scored nonsignificantly lower than CCl_4 treatment alone, but none yielded statistical significance via a one-way ANOVA with Tukey's follow-up. Figure 10*C* shows quantitative collagen-staining area from trichrome-stained sections of liver, demonstrating fibrosis in all groups of CCl_4-treated mice but no significant differences in fibrosis among groups that received cotreatment with antifibrotic compounds.

Interassay variability. Interassay variation for total OHP ^2H enrichment was calculated from three mouse liver total tissue homogenates. Ten aliquots were processed from each homogenate to the level of free amino acids and then derivatized and analyzed by GC-MS. Replicates from each homogenate had similar EM_1 values with average standard deviations for the three sets about 5.5% of the mean values, or an SD for absolute EM_1 of 0.1–0.2 MPE (Fig. 11*A*). A single outlier was noted in one group. Day-to-day variability was assessed from the same samples by derivatizing a second aliquot from each of the

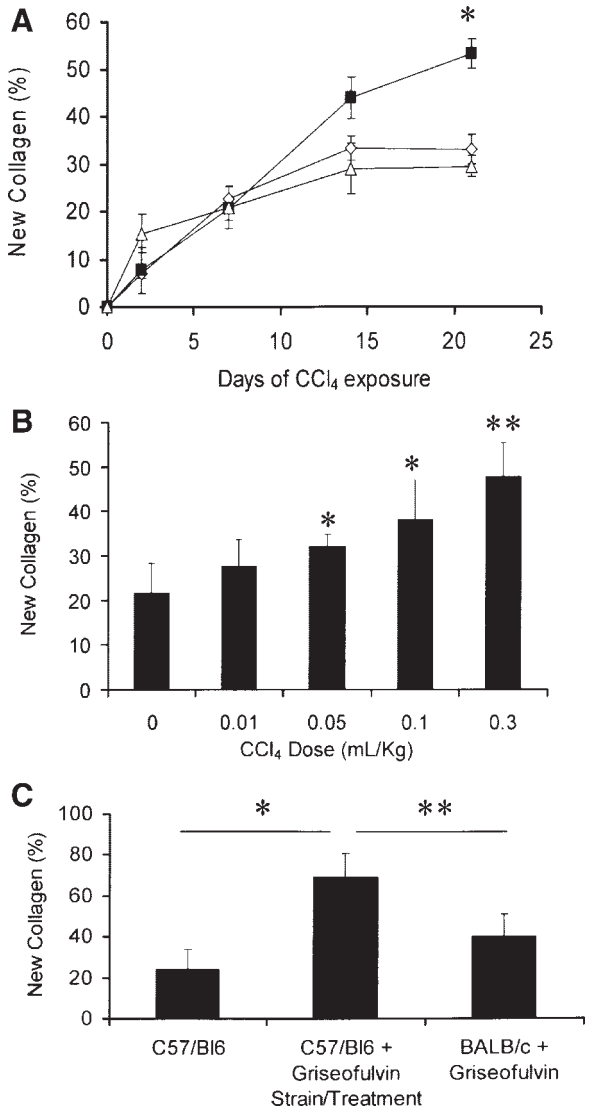

Fig. 7. Time course and dose-response curves for CCL_4 or griseofulvin administration. Interstrain differences in hepatotoxicant-induced fibrogenesis were readily observed through the measurement of total liver protein OHP enrichment. *A*: chronic exposure of 129X1/SVJ mice to 0 (△), 0.25 (◇), and 1(■) ml/kg CCl_4 produced a 1.5-fold difference in collagen fractional synthesis after 14 days of 1 ml/kg CCl_4 exposure, which achieved statistical significance (3-fold increase, $P = 0.005$, $n = 5$) after 21 days. *B*: dose response in CW mice yielded 1.5-, 1.8- and 2.2-fold increases in collagen synthesis after 1 wk of exposure to 0.05, 0.1, and 0.3 ml/kg CCl_4, respectively ($*P < 0.02$, $**P < 0.001$, $n \leq 6$). *C*: C57/Bl6J mice had a greater response to griseofulvin than did BALB/c mice after 12 days of exposure ($*P = 0.002$, $**P = 0.013$, $n \leq 5$).

original hydrolysates at a later date. Of these 30 repeated samples, one had an EM_1 value about 20% lower than the original. The remaining samples, including the outlier noted above, were all close to the initial values with an average set-to-set variation of about 3% of the EM_1 value (Fig. 11*B*).

DISCUSSION

The primary objective of this work was to develop a sensitive, relatively high-throughput method for rapidly evaluating therapeutic agents and endogenous factors that modulate fibrogenesis. A reliable and simple biomarker for assessing fibrosis and antifibrogenic agents is a long-standing goal in this field (3, 35). Rapid and quantitative measurement of tissue collagen synthesis in vivo is now possible through the use of ^2H_2O as a metabolic label. We have demonstrated that deuterium incorporation in C–H bonds of AA from isolated collagen or in OHP from total tissue protein reveals collagen synthesis rates and is sensitive to differences in rodent strain, hepatotoxicant dose, and drug treatment.

The motivation for developing a kinetic measure of fibrogenesis rate as a biomarker for assessing effects of drugs and genes is that, in principle, kinetic methods have several advantages over static measurements (18). First, changes in flux must precede changes in concentration or composition. This increases sensitivity and enables earlier detection of abnormalities. Second, the magnitude of change in flux often exceeds changes in concentration. Because biological systems typically defend against changes in pool size, increases in flux in one direction may be compensated by changes in the opposite direction. In fibrotic states, for example, when pool size of collagen is increased by an increase in collagen synthesis rate, this may be accompanied by an increase in absolute degradation rate (5), which serves to partially dampen pool size changes. Finally, small changes in rates of synthesis or breakdown can be sensitively detected, regardless of background

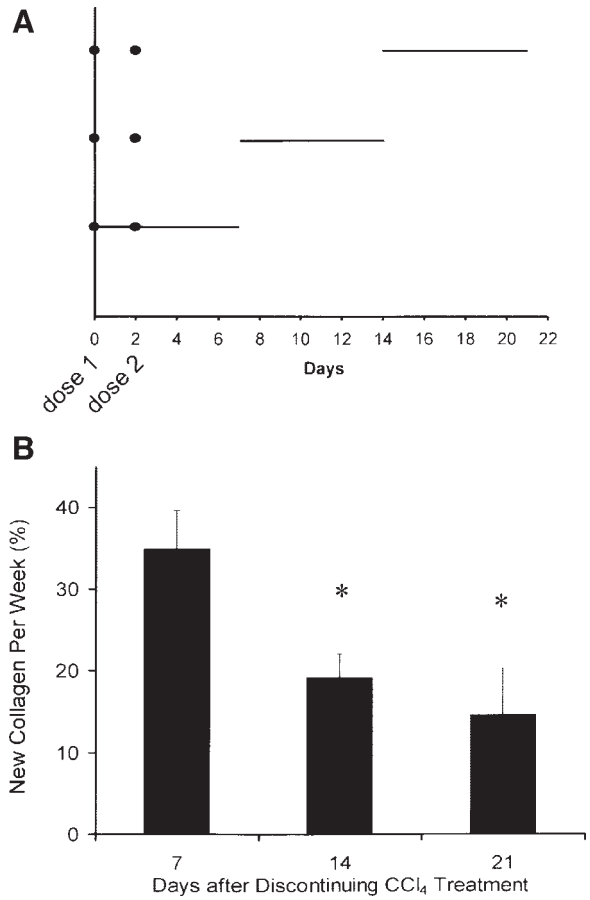

Fig. 8. Fibrogenic rate of liver diminishes rapidly after withdrawal of hepatotoxicant, as measured by total liver protein OHP synthesis. *A*: dosage time table of 0.5 ml/kg ip CCl_4 (●) and ^2H_2O (horizontal bars) administration to CW mice. This protocol was used to measure alterations in fibrogenic response as a function of time after hepatotoxicant exposure (*B*). In *B*, collagen synthesis is shown to return to normal (~20% per week) 14 days after initial exposure ($P < 0.001$, $n = 5$) and to fall slightly more, on average, after 21 days.

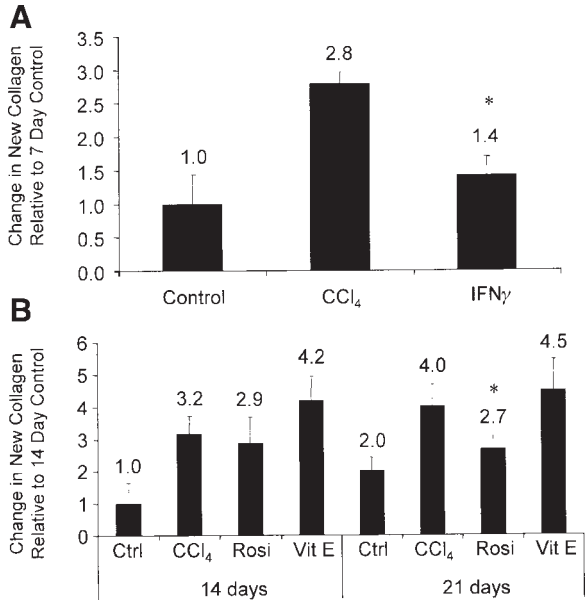

Fig. 9. Intervention in profibrotic liver injury indicates the efficacy of experimental antifibrotic therapies. *A*: IFN-γ (mouse recombinant, 50,000 U/dose once daily for 7 days at 0.2 ml/kg ip) partially suppressed CCl_4-induced fibrogenesis in CW mice (*$P < 0.001$ vs. vehicle, $n = 5$). *B*: after 14 days, dietary rosiglitazone (Rosi) did not significantly reduce CCl_4-induced fibrogenesis but did suppress fibrogenesis after 21 days (*$P < 0.001$, **$P = 0.004$ vs. control diet, $n = 5$ CW mice). Tocopherol (Vit E) administration to CCl_4-treated CW mice did not reduce hepatic fibrogenesis but rather resulted in a nonsignificant increase in hepatic fibrogenesis after 14 and 21 days, relative to CCl_4 treatment alone.

pool size, since only what is new is measured by isotopic labeling (40, 18). When a large or slowly turning over background pool is present, kinetic measurements are therefore much more sensitive to change than measures of pool size.[1] This general principle is supported by the data presented. Significant alterations in collagen synthesis were measurable after only a few days of treatment.

OHP from total tissue protein proved to be the most useful approach for measuring tissue fibrogenesis. Isolation of type I collagen was not amenable to high throughput, in addition to introducing potential bias by isolation of specific collagen conformations (e.g., monomeric vs. dimeric collagen, Fig. 3). Use of total protein OHP avoids potential biases and is capable of much higher throughput. Investigators have used total protein OHP for decades as a measure of tissue collagen content, because OHP is almost exclusively found in collagen (24). Other proteins are known to contain small numbers of hydroxylated proline residues (23, 29, 30, 31), but these proteins contribute negligibly to total protein OHP relative to collagen, because collagen is both much more abundant than other OHP-containing proteins and has a much higher OHP content per molecule (11). The parallel kinetic behaviors of collagen-bound alanine, collagen-bound OHP, and total protein OHP in rat liver (Fig. 6) are consistent with this conclusion.

Use of OHP to measure collagen synthesis required solution of a technical issue, however. Correct interpretation of ^2H enrichment in OHP is potentially problematic, since proline does not behave as a classically nonessential AA but has been reported (4) to arise largely from scavenging pathways (reutilization of proteolytically derived proline) in avian species.

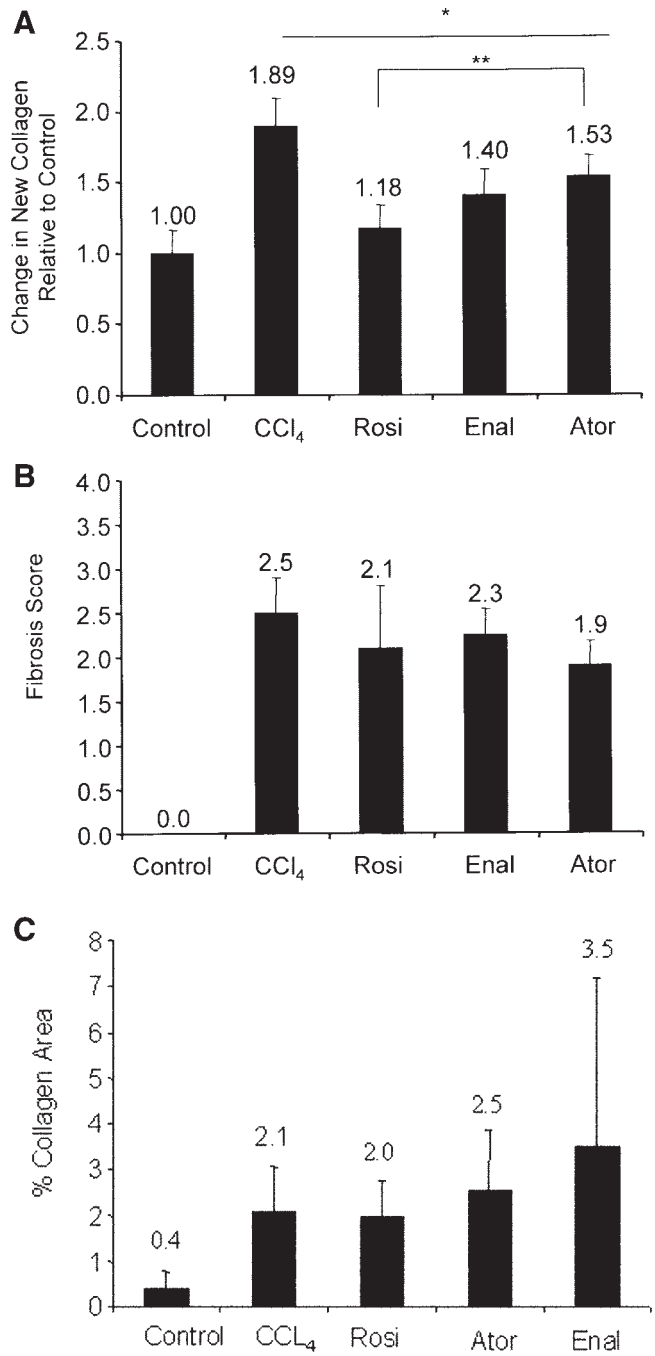

Fig. 10. After 21 days of ^2H_2O and the given treatment, fibrogenesis was more informative than histological metrics of fibrosis. *A*: rosiglitazone (Rosi), enalapril (Enal), or atorvastatin (Ator) reduced CCl_4-stimulated hepatic fibrogenesis (*$P < 0.05$) to varying extents (**$P < 0.05$, Rosi vs. Ator). *B*: pathology scoring for fibrotic index, as described in text. No significant differences among treatment groups of animals receiving CCl_4 were detected by one-way ANOVA. *C*: collagen staining area in means (SD) in trichrome-stained liver sections. No significant differences among treatment groups of animals receiving CCl_4 were detected by one-way ANOVA.

[1] A hypothetical example may help to make this point. If the liver contains 100 units of collagen at *time 0*, this may increase to 106 units after 1 wk in the presence of a fibrogenic stimulus, whereas a successful therapy might reduce this to 102 units. No assay of pool size can reliably distinguish between 106 and 102 units, but a kinetic assay (which measures "what is new") can readily distinguish between 6 and 2 newly synthesized units.

A

Liver homogenate 1		Liver homogenate 2		Liver homogenate 3	
Replicate	Ave EM1	Replicate	Ave EM1	Replicate	Ave EM1
1	1.79%	1	2.40%	1	2.56%
2	1.62%	2	2.36%	2	2.62%
3	1.93%	3	2.23%	3	2.51%
4	1.86%	4	2.44%	4	2.43%
5	1.99%	5	2.41%	5	2.49%
6	1.81%	6	2.42%	6	2.51%
7	1.87%	7	2.38%	7	2.53%
8	1.90%	8	2.34%	8	2.51%
9	1.95%	9	2.26%	9	2.33%
10	1.15%	10	2.36%	10	1.95%
Average	1.79%	Average	2.36%	Average	2.45%
Std dev	0.25%	Std dev	0.07%	Std dev	0.19%
[If omit outlier sample 10]					
Average	1.86%				
Std dev	0.11%				

B

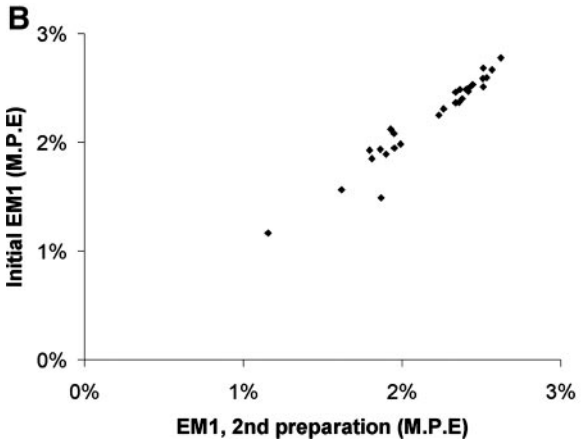

Fig. 11. Data reproducibility. *A*: 3 homogenates were made of mouse livers from animals on different treatments, but all were given deuterated water for 3 wk. Each homogenate was split 10 ways, and the samples were hydrolyzed to amino acids. Part of each hydrolysate was derivatized to allow analysis of OHP by mass spectrometry. EM_1 values (mole percent excess, MPE) for the 10 replicates of each homogenate are listed. For *homogenate 1*, a revised average was also calculated, omitting an outlying value (*sample 10* is >2.5 standard deviations from the mean). *B*: a second aliquot from each of the original 30 hydrolysates in *A* was derivatized and assayed at a later date. The 2 values for each hydrolysate are plotted against each other.

Our observations with ^2H_2O-derived ^2H labeling of OHP in mammalian liver collagen parallel these findings. Comparison of EM_1 in alanine and OHP isolated from the same protein molecules (Fig. 5) demonstrates that the number of labeled hydrogen atoms in alanine is ~2.5 times greater than in OHP. Mass isotopomeric distributions in alanine, as well as asymptotic enrichments in alanine in fully turned over proteins (9, 13), consistently indicate complete labeling of C–H bonds (i.e., $n = 4$). The lower ^2H enrichments in OHP therefore indicate that most OHP did not derive from de novo synthesized proline in the cell. On average, OHP behaves as though it contains ~1.5 C–H bonds incorporating deuterium. This value represents the combination of both the number of metabolically exchangeable, stably bound C–H bonds (n) in de novo synthesized proline and the dilution from unlabeled, reutilized proline pools (Fig. 1). Clearly, in the normal rat HSC, as in avian collagen synthesizing cells (4), the majority of proline-tRNA used for collagen synthesis derives directly from proteolytically derived proline in the cell, rather than from proline that is mixed in the rapidly synthesized, general cellular pool. Importantly, CCl_4 administration had no effect on the origins of local proline pools in the tissue (Fig. 5) or on the number of exchanging hydrogen atoms in de novo synthesized proline molecules (based on MIDA calculations).

Another technical point relates to sample preparation. Use of OHP as the final analyte allowed sample preparation to be optimized for throughput and reproducibility. Tissue homogenization, protein precipitation, hydrolysis, and derivatization procedures were adapted for high-throughput, parallel processing formats. The bead mill provided a means to homogenize samples in lieu of the Polytron tissue homogenizer, permitting parallel sample processing at this step and eliminating the potential for sample cross-contamination. For all subsequent sample handling steps, including protein precipitation and hydrolysis, the Multi-Tier plate system in a 96-well format was used. This allowed use of programmable, multichannel pipettors for all liquid handling, reducing sample preparation time considerably.

Strain- and species-dependent differences in response to profibrotic hepatotoxicants were readily apparent. Among the laboratory animals tested, the CW mouse exhibited the most sensitive fibrogenic response to CCl_4 treatment, followed by the SD rat and the 129X1/SVJ mouse. Investigators have previously reported differences between BALB/c and C57/Bl6J mouse strains for response to the antifungal agent griseofulvin (16). Our observations are consistent with this finding in that dietary griseofulvin produced a 1.7-fold higher fibrogenic response in C57/Bl6J mice than in BALB/c mice after 12 days (Fig. 7*C*).

The goal of developing an approach for rapid evaluation of therapeutic or toxic agents is strongly supported by the results reported presently. Two well-established inhibitors of HSC activation, the cytokine IFN-γ and the PPARγ agonist rosiglitazone, showed significant activity against CCl_4-induced stimulation of collagen synthesis after coadministration of either compound. IFN-γ produced significant inhibition of fibrogenesis after 1 wk, whereas rosiglitazone did not exert significant effects until after 3 wk of continuous treatment (Figs. 9 and 10). We also tested an angiotensin-converting enzyme inhibitor, enalapril, since this class has been reported to have antifibrogenic actions in various tissues (17, 27). Enalapril significantly reduced collagen synthesis to a modest extent when coadministered with CCl_4 (Fig. 10). Another agent, the hydroxyl-methyl-glutaryl-CoA reductase inhibitor atorvastatin, also caused a modest (20%) reduction in collagen synthesis when coadministered with CCl_4 for 21 days. Statins have previously been reported (12, 43) to reduce fibrogenesis by inhibiting a key isoprenylation event in the small GTPase RhoA and have been shown to reduce fibrogenic activity in vivo in a guinea pig model of pulmonary fibrosis (39). Our findings represent the first evidence that atorvastatin has in vivo antifibrotic activity in liver. In contrast, high-dose vitamin E administration did not reduce, and may even have increased, CCl_4-induced collagen synthesis, perhaps by pro-oxidant actions at high doses (7, 8, 44).

Comparison of the kinetic measure (collagen synthesis) to a standard static measure (histological trichrome staining of liver slides for collagen content) confirmed the greater sensitivity and reproducibility of the kinetic approach. CCl_4 treatment for 21 days resulted in elevated histological scores and quantitative collagen staining areas in all groups. No statistically significant

differences among treatment groups were observed, however, although rosiglitazone, enalapril, and atorvastatin all showed nonsignificantly lower staining scores at 21 days. In contrast, the results with ^2H_2O-measured collagen synthesis exhibited a considerably lower standard deviation and were highly significant statistically for these therapeutic agents. A general correlation between new collagen synthesis (f) and histological score was observed ($r^2 = 0.3$, $P < 0.05$) across all samples, supporting a relationship between the kinetic measurement and this standard biological index of fibrosis. Direct measurement of collagen synthesis was clearly much more sensitive than standard histological techniques, however, when screening for therapeutic activity of antifibrotic agents.

The measured intra-assay and interassay CV values were moderate. The analytic CV going from homogenized liver to mass spectrometric results for OHP was in the range of 2–5% (0.1–0.2 MPE). Biological variability was much higher, of course, perhaps due in part to the fact that CW mice were studied. Their outbred condition mimics expected interindividual differences in human populations. Assays of fibrogenesis yielded consistently reproducible differences in small groups of animals after exposure to profibrotic toxicants and antifibrotic drugs, however.

In future work, it will be worthwhile to consider factors that may confound measurements of fibrogenesis. Diet, age, species, strain, gender, source tissue, treatment regimens, and different disease models all may influence fibrotic response as well as the proper interpretation of alterations in fibrogenesis. The isotopic distribution of ^2H in OHP will need to be confirmed in various physiological states, along with comparisons between fibrogenic response and classic metrics of fibrotic disease (e.g., histopathology), to provide assurance that this approach remains generally valid as an assay of collagen dynamics.

In summary, a heavy water labeling technique has been developed for sensitive measurement of hepatic fibrogenic activity. OHP from total tissue proteins can be used and exhibits consistent ^2H incorporation from ^2H_2O in basal and CCl_4-stimulated conditions, while allowing analysis with a high-throughput, 96-well plate analytic format. This approach is capable of detecting subtle differences in collagen synthesis as a function of strain, dose, duration of exposure, and treatment with antifibrogenic drugs. Accordingly, the approach described presently may represent the basis for a rapid, sensitive, and quantitative in vivo platform for evaluating hepatic antifibrotic agents and investigating genes or endogenous factors that modulate fibrogenesis.

ACKNOWLEDGMENTS

We are grateful to Holly Turner for performing many of the animal handling responsibilities and to Ablatt Mashut and Chancy Fessler for processing GC-MS samples.

GRANTS

These studies were funded by KineMed, Inc., and by University of California Discovery Program (Bio Star) Grant Biostar02-10294 (to M. K. Hellerstein).

REFERENCES

1. **Babraj J, Cuthbertson DJ, Rickhuss P, Meier-Augenstein W, Smith K, Bohe J, Wolfe RR, Gibson JN, Adams C, Rennie MJ.** Sequential extracts of human bone show differing collagen synthetic rates. *Biochem Soc Trans* 30: 61–65, 2002.
2. **Baroni GS, D'Ambrosio L, Curto P, Casini A, Mancini R, Jezequel AM, Benedetti A.** Interferon γ decreases hepatic stellate cell activation and extracellular matrix deposition in rat liver fibrosis. *Hepatology* 23: 1189–1199, 1996.
3. **Bataller R, Brenner DA.** Liver fibrosis. *J Clin Invest* 115: 209–218, 2005.
4. **Berthold HK, Hachey DL, Reeds PJ, Thomas OP, Hoeksema S, Klein PD.** Uniformly ^{13}C-labeled algal protein used to determine amino acid essentiality in vivo. *Proc Natl Acad Sci USA* 88: 8091–8095, 1991.
5. **Bishop JE, Rhodes S, Laurent GJ, Low RB, Stirewalt WS.** Increased collagen synthesis and decreased collagen degradation in right ventricular hypertrophy induced by pressure overload. *Cardiovasc Res* 28: 1581–1585, 1994.
6. **Bissell DM.** Hepatic fibrosis as wound repair: a progress report. *J Gastroenterol* 33: 295–302, 1998.
7. **Bowry VW, Ingold KU, Stocker R.** Vitamin E in human low-density lipoprotein. When and how this antioxidant becomes a pro-oxidant. *Biochem J* 288: 341–344, 1992.
8. **Bowry VW, Mohr D, Cleary J, Stocker R.** Prevention of tocopherol-mediated peroxidation in ubiquinol-10-free human low density lipoprotein. *J Biol Chem* 270: 5756–5763, 1995.
9. **Busch R, Kim YK, Neese RA, Schade-Serin V, Collins D, Awada M, Gardner JL, Beysen C, Marino MM, Misell LM, Hellerstein MK.** Measurement of protein turnover rates by heavy water labeling of nonessential amino acids. *Biochim Biophys Acta* 1760: 730–744, 2006.
10. **Chen JL, Peacock E, Samady W, Turner SM, Neese RA, Hellerstein MK, Murphy EJ.** Physiologic and pharmacologic factors influencing glyceroneogenic contribution to triacylglyceride glycerol measured by mass isotopomer distribution analysis. *J Biol Chem* 280: 25396–25402, 2005.
11. **Colley KJ, Baenziger JU.** Identification of the post-translational modifications of the core-specific lectin. The core-specific lectin contains hydroxyproline, hydroxylysine, and glucosylgalactosylhydroxylysine residues. *J Biol Chem* 262: 10290–10295, 1987.
12. **Eberlein M, Heusinger-Ribeiro J, Goppelt-Struebe M.** Rho-dependent inhibition of the induction of connective tissue growth factor (CTGF) by HMG CoA reductase inhibitors (statins). *Br J Pharmacol* 133: 1172–1180, 2001.
13. **Fanara P, Turner S, Busch R, Killion S, Awada M, Turner H, Mahsut A, Laprade KL, Stark JM, Hellerstein MK.** In vivo measurement of microtubule dynamics using stable isotope labeling with heavy water. Effect of taxanes. *J Biol Chem* 279: 49940–49947, 2004.
14. **Friedman SL.** Molecular regulation of hepatic fibrosis, an integrated cellular response to tissue injury. *J Biol Chem* 275: 2247–2250, 2000.
15. **Galli A, Crabb DW, Ceni E, Salzano R, Mello T, Svegliati-Baroni G, Ridolfi F, Trozzi L, Surrenti C, Casini A.** Antidiabetic thiazolidinediones inhibit collagen synthesis and hepatic stellate cell activation in vivo and in vitro. *Gastroenterology* 122: 1924–1940, 2002.
16. **Gant TW, Baus PR, Clothier B, Riley J, Davies R, Judah DJ, Edwards RE, George E, Greaves P, Smith AG.** Gene expression profiles associated with inflammation, fibrosis, and cholestasis in mouse liver after griseofulvin. *EHP Toxicogenomics* 111: 37–43, 2003.
17. **Guo G, Morrissey J, McCracken R, Tolley T, Liapis H, Klahr S.** Contributions of angiotensin II and tumor necrosis factor-α to the development of renal fibrosis. *Am J Physiol Renal Physiol* 280: F777–F785, 2001.
18. **Hellerstein MK.** In vivo measurement of fluxes through metabolic pathways: the missing link in functional genomics and pharmaceutical research. *Annu Rev Nutr* 23: 379–402, 2003.
19. **Hellerstein MK, Hoh RA, Hanley MB, Cesar D, Lee D, Neese RA, McCune JM.** Subpopulations of long-lived and short-lived T cells in advanced HIV-1 infection. *J Clin Invest* 112: 956–966, 2003.
20. **Hellerstein MK, Neese RA.** Mass isotopomer distribution analysis at eight years: theoretical, analytic, and experimental considerations. *Am J Physiol Endocrinol Metab* 276: E1146–E1170, 1999.
21. **Hellerstein MK, Neese RA, Kim YK, Schade-Serin V, Collins ML.** Measurement of synthesis rates of slow-turnover proteins from ^2H_2O incorporation into non-essential amino acids (NEAA) and application of mass isotopomer distribution analysis (MIDA) (Abstract). *FASEB J* 16: A256, 2002.
22. **Koletzko B, Sauerwald T, Demmelmair H.** Safety of stable isotope use. *Eur J Pediatr* 156, *Suppl* 1: S12–S17, 1997.

23. **Mays C, Rosenberry TL.** Characterization of pepsin-resistant collagen-like tail subunit fragments of 18S and 14S acetylcholinesterase from *Electrophorus electricus*. *Biochemistry* 20: 2810–2817, 1981.
24. **Mays PK, McAnulty RJ, Laurent GJ.** Age-related changes in lung collagen metabolism. A role for degradation in regulating lung collagen production. *Am Rev Respir Dis* 140: 410–416, 1989.
25. **Messmer BT, Messmer D, Allen SL, Kolitz JE, Kudalkar P, Cesar D, Murphy EJ, Koduru P, Ferrarini M, Zupo S, Cutrona G, Damle RN, Wasil T, Rai KR, Hellerstein MK, Chiorazzi N.** In vivo measurements document the dynamic cellular kinetics of chronic lymphocytic leukemia B cells. *J Clin Invest* 115: 755–764, 2005.
26. **Neese RA, Misell LM, Turner S, Chu A, Kim J, Cesar D, Hoh R, Antelo F, Strawford A, McCune JM, Christiansen M, Hellerstein MK.** Measurement in vivo of proliferation rates of slow turnover cells by ^2H_2O labeling of the deoxyribose moiety of DNA. *Proc Natl Acad Sci USA* 99: 15345–15350, 2002.
27. **Pahor M, Bernabei R, Sgadari A, Gambassi G Jr, Lo Giudice P, Pacifici L, Ramacci M, Lagrasta C, Olivetti G, Carbonin P.** Enalapril prevents cardiac fibrosis and arrhythmias in hypertensive rats. *Hypertension* 18: 148–157, 1991.
28. **Parks EJ, Krauss RM, Christiansen MP, Neese RA, Hellerstein MK.** Effects of a low-fat, high-carbohydrate diet on VLDL-triglyceride assembly, production, and clearance. *J Clin Invest* 104: 1087–1096, 1999.
29. **Patthy L.** Is lung surfactant protein a lectin-collagen hybrid? *Nature* 325: 490, 1987.
30. **Porter RR, Reid KB.** The biochemistry of complement. *Nature* 275: 699–704, 1978.
31. **Rosenbloom J.** Elastin: an overview. *Methods Enzymol* 144: 172–196, 1987.
32. **Sato K, Guo YH, Feng J, Sugiyama S, Ichinomiya M, Tsukamasa Y, Minegishi Y, Sakata A, Komiya K, Yamasaki Y, Nakamura Y, Ohtsuki K, Kawabata M.** Direct fractionation of proteins in particle-containing feedstocks by a filter paper pieces-based DEAE-cellulose column chromatography. Rapid, robust and low-cost capturing procedure for protein. *J Chromatogr A* 811: 69–76, 1998.
33. **Sato K, Tanahashi-Shiina T, Jun F, Watanabe-Kawamura A, Ichinomiya M, Minegishi Y, Tsukamasa Y, Nakamura Y, Kawabata M, Ohtsuki K.** Simple and rapid chromatographic purification of type V collagen from a pepsin digest of porcine intestinal connective tissue, an unmanageable starting material for conventional column chromatography. *J Chromatogr B Analyt Technol Biomed Life Sci* 790: 277–283, 2003.
34. **Schacker TW, Nguyen PL, Beilman GJ, Wolinsky S, Larson M, Reilly C, Haase AT.** Collagen deposition in HIV-1 infected lymphatic tissues and T cell homeostasis. *J Clin Invest* 110: 1133–1139, 2002.
35. **Schuppan D, Porov Y.** Hepatic fibrosis: from bench to bedside. *J Gastroenterol Hepatol* 17, *Suppl* 3: S300–S305, 2002.
36. **Shi Z, Wakil AE, Rockey DC.** Strain-specific differences in mouse hepatic wound healing are mediated by divergent T helper cytokine responses. *Proc Natl Acad Sci USA* 94: 10663–10668, 1997.
37. **Strawford A, Antelo F, Christiansen M, Hellerstein MK.** Adipose tissue triglyceride turnover, de novo lipogenesis, and cell proliferation in humans measured with ^2H_2O. *Am J Physiol Endocrinol Metab* 286: E577–E588, 2004.
38. **Tamayo RP, Montfort I, Pardo A.** What controls collagen resorption in vivo? *Med Hypotheses* 6: 711–726, 1980.
39. **Tan A, Levrey H, Dahm C, Polunovsky VA, Rubins J, Bitterman PB.** Lovastatin induces fibroblast apoptosis in vitro and in vivo. A possible therapy for fibroproliferative disorders. *Am J Respir Crit Care Med* 159: 220–227, 1999.
40. **Turner SM, Hellerstein MK.** Emerging applications of kinetic biomarkers in preclinical and clinical drug development. *Curr Opin Drug Discov Devel* 8: 115–126, 2005.
41. **Turner SM, Murphy EJ, Neese RA, Antelo F, Thomas T, Agarwal A, Go C, Hellerstein MK.** Measurement of TG synthesis and turnover in vivo by ^2H_2O incorporation into the glycerol moiety and application of MIDA. *Am J Physiol Endocrinol Metab* 285: E790–E803, 2003.
42. **Vater CA, Harris ED Jr, Siegel RC.** Native cross-links in collagen fibrils induce resistance to human synovial collagenase. *Biochem J* 181: 639–645, 1979.
43. **Watts KL, Spiteri MA.** Connective tissue growth factor expression and induction by transforming growth factor-β is abrogated by simvastatin via a Rho signaling mechanism. *Am J Physiol Lung Cell Mol Physiol* 287: L1323–L1332, 2004.
44. **Witting PK, Bowry VW, Stocker R.** Inverse deuterium kinetic isotope effect for peroxidation in human low-density lipoprotein (LDL): a simple test for tocopherol-mediated peroxidation of LDL lipids. *FEBS Lett* 375: 45–49, 1995.